Journal of Luminescence 147 (2014) 121–126

Contents lists available at ScienceDirect

Journal of Luminescence

journal homepage: www.elsevier.com/locate/jlumin

Infrared luminescence of annealed germanosilicate layers

M.S. Tokay [a], E. Yasar [a,*], S. Ağan [a], A. Aydınlı [b]

[a] Department of Physics, Kırıkkale University, 71450 Kırıkkale, Turkey
[b] Department of Physics, Bilkent University, 06800 Ankara, Turkey

ARTICLE INFO

Article history:
Received 18 July 2013
Received in revised form
21 October 2013
Accepted 25 October 2013
Available online 8 November 2013

Keywords:
Infrared luminescence
Germanosilicate
Photoluminescence spectroscopy
Raman scattering
Annealing

ABSTRACT

In the light of growing importance of semiconductor nanocrystals for photonics, we report on the growth and characterization of annealed germanosilicate layers used for Ge nanocrystal formation. The films are grown using plasma enhanced chemical vapor deposition (PECVD) and post-annealed in nitrogen at temperatures between 600 and 1200 °C for as long as 2 h. Transmission electron microscopy (TEM), Raman scattering and photoluminescence spectroscopy (PL) has been used to characterize the samples both structurally and optically. Formation of Ge precipitates in the germanosilicate layers have been observed using Raman spectroscopy for a variety of PECVD growth parameters, annealing temperatures and times. Ge–Ge mode at ~300 cm^{-1} is clearly observed at temperatures as low as 700 °C for annealing durations for 45 min. Raman results indicate that upon annealing for extended periods of time at temperatures above 900 °C; nanocrystals of few tens of nanometers in diameter inside the oxide matrix and precipitation and interdiffusion of Ge, forming SiGe alloy at the silicon and oxide interface take place. Low temperature PL spectroscopy has been used to observe luminescence from these samples in the vicinity of 1550 nm, an important wavelength for telecommunications. Observed luminescence quenches at 140 K. The photoluminescence data displays three peaks closely interrelated at approximately 1490, 1530 and 1610 nm. PL spectra persist even after removing the oxide layer indicating that the origin of the infrared luminescent centers are not related to the Ge nanocrystals in the oxide layer.

1. Introduction

There is currently great interest in nanometer sized Si and Ge structures following the observation of the efficient visible photoluminescence (PL) from porous Si [1], since this could open new possibilities for indirect gap semiconductors as new materials in optoelectronic applications. In particular, PL properties of Si nanocrystals (nc-Si) have widely been studied and the relationship between the size of nc-Si and the PL peak energy has been revealed experimentally [2]. Many approaches to the realization of Si nanocrystals in a variety of matrices have been proposed. Si nanocrystals in insulating matrices, such as SiO_2, are also considered candidates for future memory devices [3]. Intense work is under way to realize a Si laser [4]. Silicon nanocrystals in SiO_2 typically form at relatively high temperatures, such as 1100 °C, when annealed for 1 h or more and exhibit tunable photoluminescence due to size controlled nanocrystals formed by appropriate annealing conditions.

On the other hand, germanium (Ge) also is an indirect band gap semiconductor similar to silicon in many respects except for a smaller band gap. Ge containing SiO_2 thin films can be obtained through, among many different techniques, ion implantation or plasma enhanced chemical vapor deposition (PECVD) of germanosilicate layers [5,6] to name a few. However, Ge nanocrystals form at much lower annealing temperatures and durations as opposed to Si nanocrystals. While annealing temperatures of 800 °C and durations of a few minutes is typical to obtain Ge nanocrystals, Ge clusters of 2–3 nm sizes have been claimed to have formed even at annealing temperatures as low as 300 °C when annealed for 30 min [7]. However, lattice fringes of these nanocrystals have not been observed casting shadow on their crystallinity. Both TEM and Raman scattering have been employed to observe the formation of Ge nanocrystals in single and multilayers [8]. Extensive photoluminescence work yielded mixed results. Dutta [9] reported observing blue luminescence from Ge nanocrystals and claimed that PL is due to quantumconfined electronic transitions despite insufficient data. Paine et al. [10] have observed photoluminescence at 580 nm obtained from samples by H_2 reduced $Si_{0.6}Ge_{0.4}O_2$ and postannealed 750 °C which they attributed to Ge nanocrystals. Ge nanocrystals prepared by the sol–gel method in SiO_2 and three photoluminescence peaks in the range of 2.0–2.3 eV were attributed to Ge nanocrystals [11]. Maeda [7] has studied Ge nanocrystals in SiO_2 prepared by the cosputtering method and have observed both blue (3.1 eV) and visible (2.2 eV) photoluminescence and analyzed the data considering the quantum confinement model as well as Ge: E' luminescence centers in glasses

* Corresponding author. Tel.: +90 318 357 42 42; fax: +90 318 357 24 61.
E-mail addresses: erdemyasar@kku.edu.tr, erdem.yasar@gmail.com (E. Yasar).

0022-2313/$ - see front matter © 2013 Elsevier B.V. All rights reserved.
http://dx.doi.org/10.1016/j.jlumin.2013.10.060

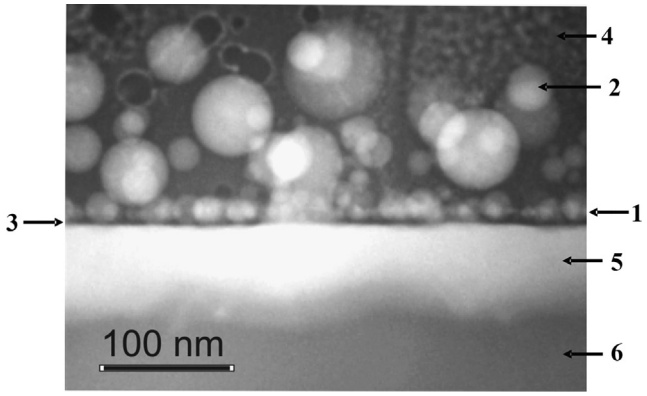

Fig. 1. Dark field STEM image of a sample annealed at 1000 °C for 1 h. Ge nanocrystals are formed in the vicinity of the interface (number 1 and 2). Note the presence of two layers with two distinct average sizes of Ge nanocrystals. A nanocrystal free SiO_2 interface oxide (number 3) and oxide close to the surface devoid of Ge nanocrystals, (number 4) is observed. Ge diffuses into Si substrate for an average thickness of 50 nm and Si substrate (number 5). Si substrate is also indicated (number 6).

and structural transitions of nanocrystal Ge, favoring the former model. Takeoka [12] has studied the near infrared photoluminescence in the range of 0.88–1.54 eV from Ge nanocrystals prepared by the cosputtering method and concluded that the observed luminescence is due to radiative recombination of electron–hole pair confined in Ge nanocrystals. Torchynska et al. [13] have studied Ge nanocrystals in SiO_2 and have concluded that all bands in the range of 1.6–2.35 eV are due to defects in SiO_x whereas PL bands in the range of 0.75–0.85 eV are attributed to excitonic recombination inside Ge nanocrystals. It is thus clear from the literature that origin of photoluminescence from Gedoped silicate layers is still not clear. Much work has been devoted to study the electrical properties of Ge nanocrystals in SiO_2 matrices [14]. Charging and discharging of Ge nanocrystals have been studied for flash memory applications. The possibility of charge storage in quantized levels of Ge nanocrystals has been shown [15].

In this work, Ge nanocrystals in SiO_x matrix were prepared by plasma enhanced chemical vapor deposition of SiO_x doped with Ge followed by postannealing of these layers. Both short term anneals as well as prolonged annealing has been carried out in nitrogen environment in the range of temperatures from 600 to 1200 °C. Both the formation of Ge nanocrystals in the oxide matrix as well as diffusion and intermixing of Ge with Si in the substrate and the formation of SiGe alloy have been observed by TEM and Raman spectroscopy. Photoluminescence in the visible as well as in the near infrared is studied both at low and room temperatures. Photoluminescence in the near infrared is studied in detail because of the important optical communication wavelength region of 1.3–1.5 μm. Persistence of the photoluminescence even after the removal of the oxide layer containing the Ge nanocrystals suggests that, Ge islands on the Si substrate and SiGe alloy that forms at the interface of the oxide layer with the Si substrate, should also be considered for the origin of the observed luminescence.

2. Experimental procedure

The SiO_x:Ge films were grown in a PECVD reactor (PlasmaLab 8510C) on Si substrates using 185 sccm SiH_4 (2% in N_2), 45 sccm NH_3 and 120 sccm flow rate of GeH_4 (2% in He) as precursor gases, at a substrate temperature of 350 °C, a process pressure of 1000 mTorr under an applied RF power of 10 W. The samples were then annealed under nitrogen environment in a quartz oven at temperatures ranging from 600 to 1200 °C as long as 2 h. Raman scattering experiments were carried out using a 1-m double monochromator with GaAs photomultiplier and photon counting electronics. Various lines of an Ar ion (Ar^+) laser and a 35 mW He–Ne laser at 632.8 nm were used to excite the samples. Photoluminescence spectroscopy in the infrared is carried out at low temperatures with a 50 cm single pass monochromator equipped with a large area InGaAs detector. A closed cycle refrigerator is used down to 15 K.

Cross section of the samples was observed with a transmission electron microscopy (TEM). The samples for the TEM observations were prepared by standard procedures in cross-section orientation and view edge on. Mechanical and Ar^+ thinning techniques were used to thin down the samples. Ar^+ at 5 keV incident at 9–12° was used. To minimize Ar^+ damage, the accelerating voltage was lowered down to 1 keV in the final stages of the thinning process. The structural characterization was carried out with a JEOL 2010F field-emission transmission electron microscope operated at 200 keV.

3. Results and discussion

Fig. 1 shows a crosssectional dark field STEM image for a typical PECVDgrown SiO_x:Ge films annealed at 1000 °C for 1 h. Upon annealing, crystallization of Ge is observed in the samples. TEM image shows that these nanocrystals fall into two groups. These two groups are composed of small nanocrystals with an average size of 15 nm and large nanocrystals that have an average size of 50 nm. From the TEM micrography, a 3–5 nm thick layer of oxide on the Si substrate is observed to be free of Ge nanocrystals (number 1). Furthermore, Ge is observed at the Si/SiO_x interface mixed with Si forming SiGe alloy. Thin layers or islands of Ge may also be present at the interface. It is suggested that Ge nanocrystals from GeO_2 form due to an exchange reaction with Si diffusing in from the substrate into the oxide layer forming SiO_2 and leaving elemental Ge behind [9]. The fact that Ge nanocrystals form only in the vicinity of the Si substrate seems to corroborate this mechanism. EDAX analysis of the substrate close to the Si/SiO_x interface as well as the narrow band of contrast with the Si substrate at the interface seen in the TEM images suggest the presence of Ge on and in the Si substrate. All this is indicative of diffusion of Ge through the oxide layer and the formation of the SiGe layer at the silicon substrate–oxide interface.

Fig. 2 displays the results of Raman measurements from the same samples displaying the evolution of Ge nanocrystal formation upon annealing at temperatures in the range of 600–1200 °C. As an example, we show the spectra for samples in the annealing temperature ranges of 600–1200 °C for 45 min. The spectrum remains virtually unchanged for the annealing temperatures less than 600 °C. We observe a very broad ($\sim$40 cm^{-1}) asymmetric peak centered around 291 cm^{-1} indicative of the quasiamorphous nature of the Ge for samples annealed at 600 °C dominates the spectrum. We also note that the sharp rise on the right culminates in a very small peak at 299.27 cm^{-1} mixing into the quasi-amorphous peak. Presence for this peak suggests that 600 °C is the onset of Ge crystallization as observed by Raman spectroscopy. Si substrate is observed at 520.4 cm^{-1}. If the annealing temperature is raised to 700 °C, a sharp peak at 299 cm^{-1}, now 10 cm^{-1} in width, (not shown) is accompanied by a wide shoulder on the low frequency side. The sharp peak is a clear sign of Ge nanocrystal formation accompanied by a range of smaller Ge nanostructures. We note that this peak is at a lower frequency than the Ge mode in bulk Ge. This is most likely due to phonon confinement in small crystals. This peak becomes stronger at 299.8 cm^{-1} and narrower (5.3 cm^{-1}) and the broad quasi-amorphous structure disappears

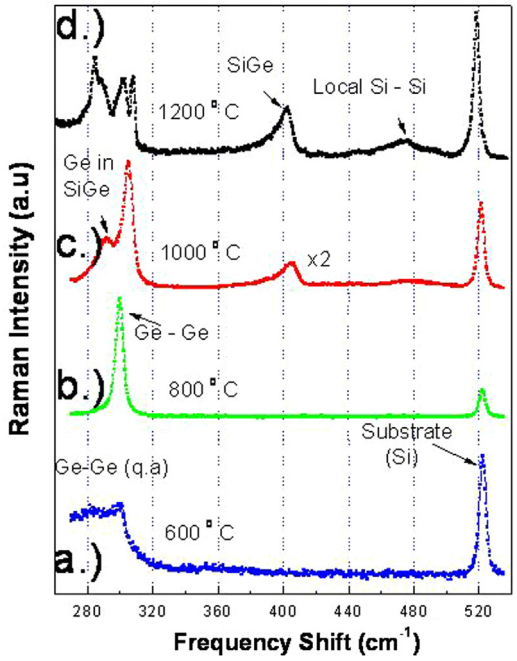

Fig. 2. Displays the Raman spectra of PECVD grown SiO_x:Ge films displaying the evolution of Ge nanocrystal formation upon annealing at temperatures in the range of 600–1200 °C from 40 to 120 min.

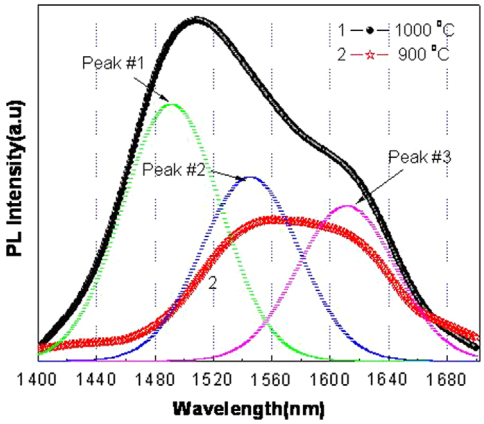

Fig. 3. Low temperature (15 K) IR PL spectra of SiO_x:Ge films annealed at 900 and 1000 °C for 45 min.

as the annealing temperature is increased up to 800 °C, Fig. 2b. At 900 °C (not shown) the Ge–Ge mode displays a double peak structure. These are located at 300.5 and 306.5 cm^{-1}. The peak at lower frequency is attributed to Ge–Ge modes of the SiGe alloy at the interface while the higher frequency component of this double peak is due to the Ge nanocrystals in the oxide layer. This assignment has been confirmed with oxide removal experiments. After the removal of the oxide only the lower frequency component remains. In addition to the features associated with Ge nanocrystals, the spectrum now displays a weak but clearly discernible asymmetric peak centered at 410 cm^{-1} indicating the formation of SiGe alloy at the oxide Si substrate interface. In fact, if the oxide layer is completely removed with dilute HF solution, the same broad peak at 410 cm^{-1} is still observable. Furthermore, a very weak and broad peak centered at 482 cm^{-1} accompanies the SiGe at 410 cm^{-1}. This peak is attributed to local Si–Si modes and is expected with the formation of SiGe alloy. Finally, the Si substrate peak observed as a sharp peak centered about 520.5 cm^{-1}.

Raman data for samples annealed at 1000 °C is shown in Fig. 2c. Two peaks associated with Ge modes down shift to 293.5 and 305.5 cm^{-1}. The asymetric peak also down shift to 405 cm^{-1} and is now clearly pronounced. The Si–Si local mode is still quite broad but slightly down shifted to 476 cm^{-1}. Si–Si mode due to the substrate remains at 521 cm^{-1}. Sample was also annealed at 1200 °C. The Ge–Ge double peaks now evolve into three peaks located approximately at 308, 302 and 285 cm^{-1}. We speculate that the broad third peak at the low frequency side of the spectrum is due to SiGe alloys of varying compositions. The SiGe peak is now located at 403 cm^{-1} and the Si–Si local mode remains at approximately the same position (474 cm^{-1}) as that in the spectrum of 1000 °C. Notably the Si substrate peak is also down shifted to 518.6 cm^{-1} suggesting that it is under stress.

Photoluminescence spectroscopy on these samples revealed very little in the visible part of the spectrum. Typically, a peak centered around 550 nm is observed and known to be due to defect states in the glassy matrix. The spectra in the near IR on the other hand have a broad peak center around 1550 nm, Fig. 3. The spectra in Fig. 3 is from two samples annealed at 1000 and 900 °C for 45 min and consists of three peaks centered ~1490(0.832 eV), ~1530(0.810 eV) and ~1610(0.770 eV) nm. The effect of annealing temperature on the infrared spectrum may be better understood if we study samples annealed for different durations. Low temperature (15 K) IR spectra from such a sample annealed at 950 °C for 40, 60 and 120 min is shown in Fig. 4. We again find a broad peak with well-defined peaks in the spectrum at ~1516 (0.817 eV), ~1524(0.813 eV) and ~1533(0.808 eV) nm, a clear blue shift of the spectra with increasing annealing duration. The data can be deconvoluted well with three Gaussian peaks.

The temperature dependence of the photoluminescence has also been studied, Fig. 5. We find that the highest intensity is obtained at the lowest temperature and as the temperature of the sample is raised during the measurement the peak intensity decreases. The signal to noise ratio detoriates as the temperature reaches 120 K and any sign of a photoluminescence signal cannot be distinguished beyond 140 K.

Several possible mechanisms may be considered to explain the data. Among these are luminescence from dislocations in the SiGe alloy, luminescence from Ge or SiGe islands in or on the Si substrate and Ge nanocrystals in the SiO_x matrix. To test the latter consideration, the oxide layer has been removed in a dilute HF solution and the photoluminescence experiment was repeated. The observed spectrum is almost identical with those obtained when the oxide layer was in fact.

Photoluminescence from Ge and SiGe islands on Si has been studied by numerous authors. Kamenev et al. [16] has studied photoluminescence from nanometer sized clusters with Ge core and SiGe shell grown on Si by molecular beam epitaxy under near Stranski–Krastanov growth mode conditions and found a broad band covered the range from 0.85 to 0.95 eV which broadens and shifts down to the range 0.65–0.90 eV as the Ge concentration increases. Talalaev et al. [17] have studied Ge/Si multilayer structures with Ge quantum dots. The observed photoluminescence spectra cover a broad range between 0.75–0.90 eV. Eberl et al. [18] measured photoluminescence characteristics of self-assembled SiGe nanostructures and observed a broad peak between 0.75 and 0.90 eV.

We have also studied the variation of the emission A band maximum intensity versus the excitation laser intensity. Excluding the saturation region at the highest intensities, the experimental data can be fitted by the simple power law of the form $I \alpha L^{\gamma}$ where I is the PL intensity, L is the excitation laser intensity and γ is a dimensionless exponent. It was found that the PL intensity at the emission band maximum increases sublinearly with respect to the excitation laser intensity Fig. 6. It is well known that for an

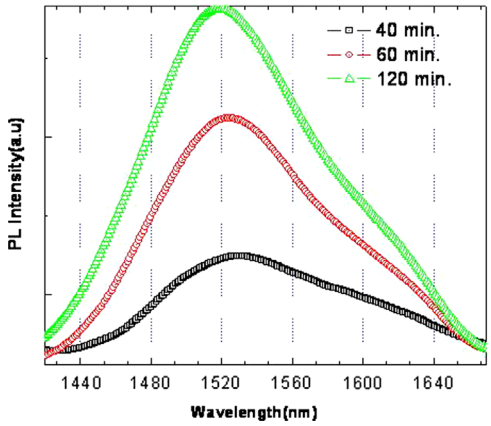

Fig. 4. Low temperature (15 K) IR PL spectra of SiO_x:Ge films annealed at 950 °C with 40, 60 and 120 min annealing times.

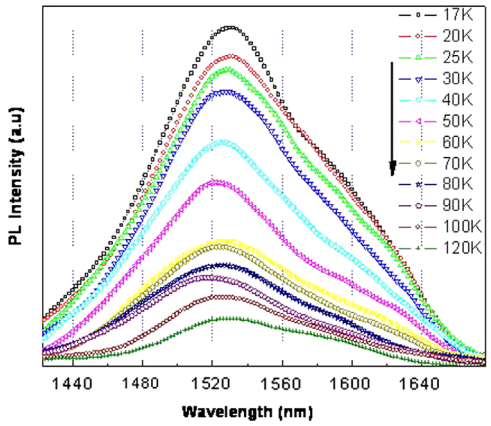

Fig. 5. Temperature dependent IR PL spectra of SiO_x:Ge films annealed at 1200 °C for 1 h under 632.8 nm excitation.

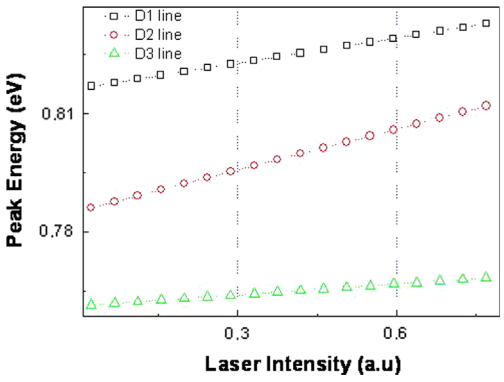

Fig. 6. Excitation intensity dependent low temperature IR PL of samples annealed at 1200 °C during 1 h.

excitation laser photon with an energy exceeding the bandgap energy E_g, the coefficient γ is generally $1<\gamma<2$ for the free and bound-exciton emission, and $\gamma \leq 1$ for free-to-bound and donor–acceptor pair recombinations [19].

Studies of the PL temperature dependence show that at high temperatures, the PL intensity drops exponentially, and the activation energies of PL thermal quenching are shown in Fig. 7 of SiO_x: Ge films annealed at 1200 °C during 1 h. The transition–temperature of 140–160 K can be understood as that the carriers transport is hopping from site to site when T < 140 K, so there is

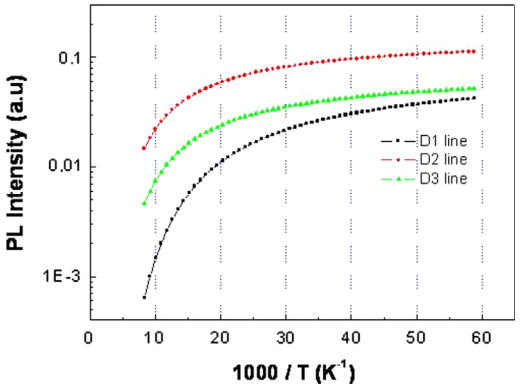

Fig. 7. Arrhenius plot of SiO_x:Ge films annealed at 1200 °C during 1 h. Temperature dependence of PL intensity at the A band of sum. The arrow shows the starting point of the intensive quenching.

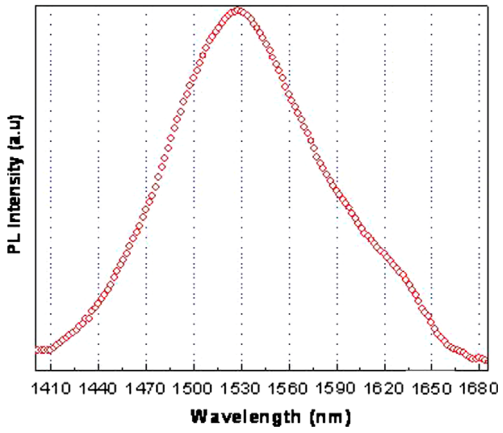

Fig. 8. PL results come from nanocrystals via removing oxide layer for the sample annealed at 1000 °C at 45 min.

not much chance for them to be captured by the nonradiative center; when temperature is increased to T > 160 K, the carriers are thermally emitted to the band edge and then are easily captured by the non-radiative recombination centers. Fig. 7 shows the temperature dependence of the A band maximum intensity as a function of the reciprocal temperature in the 11.5–81 K range. A rapid thermal quenching of the A band is observed above $T=35$ K. The experimental data for the temperature dependence of the PL intensity at the emission band maximum (I) can be fitted by the following expression:

$$I(T) = I_0 \exp\left(\frac{\Delta E}{kT}\right)$$

where I_0 is a proportionality constant, ΔE is the thermal activation energy and k the Boltzmann constant. The semilogarithmic plot of the emission band intensity as a function of the reciprocal temperature gives a straight line in the 35–81 K region. In conclusion, we have shown that the photoluminescence of Ge self-assembled quantum nanocrystals is strongly dependent on the power excitation density.

Finally, we have examined to the PL results come from nanocrystals via removing oxide layer from the sample annealed at 1000 °C at 45 min shown in Fig. 8. At 15 K maximum peak was obtained 1528 nm. There is a red shift with comparing unremoved oxide layer sample annealed at the same temperature and time.

There are several possibilities for the source of the observed IR PL form high temperature annealed Ge doped SiO_x films on Si substrates. First, Si substrate itself is known to have defect related

PL emission in this part of the spectrum. These well documented emission lines dubbed as D1 through D4 occur ~1528, 1423, 1317 and 1238 nm [20]. The physical origin of these emission lines have been studied both theoretically [21] and experimentally. Using density functional theory, it has been shown that clusters of Si with defect states may be responsible for the emitted PL. Furthermore such defectrelated lines are also observed in SiGe alloys [22]. In partially, relaxed samples some of the D lines are not observed. In totally relaxed samples all four D lines are observed with varying degrees of intensity. Secondly, PL emission from bandto-band recombination of SiGe alloys is also a possibility. PL emission from SiGe structures are observed [23] in this part of the spectra as it lies between the bandgap of Si and that of Ge. Nearband gap luminescence from SiGe alloys have been studied [24]. Low temperature spectra shows excitonic structures shifting from red to blue as the Ge content of the SiGe alloy decreases. Ge–Ge, Si–Ge and Si–Si modes of the system has been characterized as a function of SiGe composition and does not show any dispersion making it difficult to use the Raman line positions as calibration tools for the determination of composition of our films. Molecular beam epitaxy of SiGe and Ge on Si has also been attempted [25]. Ge islands growing on Si substrates show a blue shifted PL emission ~1500 nm for very low coverage. The data is explained in terms of quantum confined Ge clusters, which show PL red shifting upon increasing cluster size. Finally, interdiffusion of Ge into Si has been studied with concominant PL emission in the IR in the form of D lines [26]. As our Raman data shows the presence of SiGe in our samples our PL data seems to be consistent with defectrelated PL emission from SiGe during the interdiffusion of Ge into Si. Alternatively, PL emission from SiGe alloys is also a possibility. The data is explained in terms of quantum confined Ge clusters, which show PL red shifting upon increasing cluster size.

These localized luminescence centers likely originate from defect centers at the Ge/Si interface or defect centers inside the Ge clusters. We increased the Ge concentration in the SiO_x films. The exclusive presence of Peak1 and Peak2 emission bands in the samples containing amorphous Ge nanoclusters indicates that these amorphous clusters must play a critical role in the PL process. A possible explanation of the PL is that excitons are generated in the Ge nanoclusters or in bulk Si and then decay at defect centers that are located either within the nanocrystals or at the Si interface. The presence of Ge nanoclusters produces high energy excitons, higher than the bulk Ge band gap energy and a high density of interface states. This model has been used extensively to explain the luminescence properties from Si and Ge nanocluster systems [27]. No visible luminescence was observed from the samples, however, a broad photoluminescence peak around 1500 nm was observed at low temperatures in samples with germanium precipitates.

It is necessary to understand the enhanced PL properties of the Ge nanocrystals for possible further enhancement. It is known that the surface and/or interface states of the crystals have a great effect on their PL properties. These surface/interface states can act as either radiative or nonradiative recombination centers, consequently leading to a significant enhancement of PL intensity. Oxygen-deficient centers also can act as deep traps. Therefore, one can expect further PL enhancement if the crystal size is further decreased, the oxidation condition is optimized and/or the nonradiative defect density is decreased [28].

This broad peak (0.8–1.0 μm) is probably due to interfacial oxygen-deficient defects between the oxide and the ncGe.

Theoretically, quantum dot infrared photodetectors have been predicted to have high gain and low dark currents compared to quantum wire infrared photodetectors. It has also been reported that the PL intensity increases drastically as the size decreases. In general, the red and near-infrared PL previously observed are considered to originate from the recombination of electron–hole pairs between the widened band gap of nc-Si (quantum size effects).

4. Conclusions

In this study, nanostructures of Ge formed by precipitation of germanium in PECVD grown germanosilicate films were studied using TEM, Raman and PL spectroscopies. We have fabricated SiO_x:Ge thin films using PECVD. Cross-sectional TEM images show the formation of nanocrystal structures in SiO_x matrix and Raman scattering was used to monitor the formation of Ge nanocrystals for as-grown and nitrogen and vacuum annealed samples. Annealing results in the formation of SiGe alloy at the oxide Si interface. Photoluminescence spectra obtained from the SiO_x:Ge suggests that luminescence originates from defect centers and is not consistent with the quantum confinement based luminescence expected from Ge nanocrystals despite the fact that Raman scattering clearly points to their presence.

Annealing of SiO_x:Ge films result in of formation of Ge nanocrystals and SiGe alloy the oxide Si interface; the formation of two distinct types of structures has been verified through Raman scattering measurements and TEM micrographs.

Low temperature photoluminescence in the IR around 1500 nm has been identified as Ge islands formed at the silicon and oxide interface, an important wavelength for telecommunications. Formation of such structures by simple PECVD growth and annealing is interesting because of their potential use as infrared emitters.

Acknowledgment

We thank to Aykutlu Dana for sample growth. This work is supported by TÜBİTAK (Turkish Scientific and Technical Research Council) through contact 109T129.

References

[1] J. Pandiarajan, N. Jeyakumaran, N. Prithivikumaran, Adv. Mater. Res. 584 (2012) 290.
[2] J. Alberto, L. López, J. Carrillo López, D.E. Vázquez Valerdi, G. García Salgado, T. Díaz-Becerril, A. Ponce Pedraza, F.J. Flores Gracia, Nanoscale Res. Lett. 7 (2012) 604.
[3] C. Bonafos, M. Carrada, G. Ben Assayag, S. Schamm-Chardon, J. Groenen, A. Slaoui, P. Dimitrakis, P. Normand, Mater. Sci. Semicond. Process. 15 (2012) 615.
[4] Ding Li, Yong-Bin Chen, Ming Lu, Mater. Lett. 89 (2012) 9.
[5] N.L. Rowell, D.J. Lockwood, A. Karmous, P.D. Szkutnik, I. Berbezier, A. Ronda, Superlattices Microstruct. 44 (2008) 305.
[6] R. Xu, W. Li, J. He, Y. Sun, Ya-Dong Jiang, J. Non-Cryst. Solids 365 (2013) 37.
[7] Y. Maeda, Phys. Rev. B 51 (3) (1995) 1658.
[8] S. Agan, A. Dana, A. Aydinli, J. Phys-Condens. Matter 18 (2006) 5037.
[9] A.K. Dutta, Appl. Phys. Lett. 68 (9) (1996) 1189.
[10] D.C. Paine, C. Caragianis, T.Y. Kim, T. Shigesato, T. Ishahara, Appl. Phys. Lett. 62 (22) (1996) 2842.
[11] M. Nogami, Y. Abe, Appl. Phys. Lett. 65 (20) (1994) 2545.
[12] S. Takeoka, M. Fujii, S. Hayashi, Phys. Rev. B. 58 (12) (1998) 7921.
[13] T.V. Torchynska, A.V. Hernandez, Y. Goldstein, J. Jedrzejewskii, S. Jiménez Sandoval, J. Non-Cryst. Solids 352 (2006) 1152.
[14] H. Liu, W. Winkenwerder, Y. Liu, D. Ferrer, D. Shahrjerdi, S.K. Stanley, J.G. Ekerdt, S.K. Banerjee, IEEE Trans. Electron. Dev. 55 (12) (2008) 3610.
[15] A. Dana, I. Akça, O. Ergun, A. Aydınlı, Physica E 38 (1–2) (2007) 94.
[16] B.V. Kamenev, J.M. Baribeau, D.J. Lockwood, L. Tsybeskov, Physica E 26 (1–4) (2005) 174.
[17] V.G. Talalaev, G.E. Cirlin, A.A. Tonkikh, N.D. Zakharov, P. Werner, U. Gösele, J.W. Tomm, T. Elsaesser, Nanoscale Res. Lett. 1 (2006) 137.
[18] K. Eberl, O.G. Schmit, R. Duschl, O. Kienzle, E. Ernst, Y. Rau, Thin Solid Films 369 (1–2) (2000) 33.
[19] W. Wang, K. Wang, D. Han, Bed Poudel, Xiaowei Wang, D.Z. Wang, Baoqing Zeng, Z.F. Ren, Nanotechnology 18 (7) (2007) 5707.
[20] V. Higgs, F. Chin, X. Wang, J. Mosalski, R. Beanland, J. Phys. Condens. Matter 12 (2000) 10105.

[21] A.T. Blumenau, R. Jones, S. Öberg, P.R. Briddon, T. Frauenheim, Phys. Rev. Lett. 87 (2001) 1874041.
[22] E.A. Steinman, V.I. Vdovin, T.G. Yugova, Semicond. Sci. Technol. 14 (1999) 582.
[23] K. Terashima, T. Ikarashi, D. Tweeti, K. Miyanaga, T. Tatsumi, M. Tajima, Appl. Phys. Lett. 65 (1994) 601.
[24] J. Weber, M. Alonso, Phys. Rev. B 40 (1989) 5683.
[25] J.P. Noël, N.L. Rowell, D.C. Houghton, D.D. Perovic, Appl. Phys. Lett. 61 (1992) 690.
[26] K. Shum, P.M. Mooney, J.O. Chu, Appl. Phys. Lett. 71 (1997) 1074.
[27] A.A. Shklyaev, M. Ichikawa, Appl. Phys. Lett. 80 (2002) 1432.
[28] W.Z. Wang, B. Poudel, J.Y. Huang, D.Z. Wang, S. Kunwar, Z.F. Ren, Nanotechnology 16 (2005) 1126.